



# Study of The Influence of Physical Factors on The Formation of Superhard Nanocomposite Coatings Zr-Ti-Si-N And Ti-Hf-Si-N and Their Properties

Makhmudov N A<sup>1</sup> and Umarov A V<sup>2,3\*</sup>

<sup>1</sup>Academy of the armed forces of the republic of Uzbekistan<sup>4</sup>, Uzbekistan

<sup>2</sup>Tashkent State Transport University, Tashkent, Uzbekistan

<sup>3</sup>Tashkent University of Applied Science<sup>2</sup>, Uzbekistan

\*Corresponding author: Umarov A V, Department of Applied Science, Tashkent State Transport University, Tashkent, Uzbekistan.

Received Date: July 03, 2023

Published Date: July 11, 2023

## Abstract

This article considers the physical factors that affect the formation of superhard nanocomposite coatings Zr-Ti-Si-N and Ti-Hf-Si-N, and investigates the friction properties, adhesive and cohesive strength of nanocomposite coatings. In all experiments, the conditions for the processes of destruction of coatings under the action of a diamond indenter were studied.

**Keywords:** Nanocomposition; Friction; Wear; Multilayer coatings; Tribological properties.

## Introduction

Research of micro and nanostructured objects is the fastest growing area in modern solid state physics and materials science. An ultrafine structure can provide a significant modification, and in some cases leads to a unique change in the properties of materials [1-4]. From a physical point of view, the transition to a nanostate is associated with the appearance of size effects, which should be understood as a complex of phenomena associated with a change in the properties of a substance due to the coincidence of the size of a microstructure block and a certain critical length characterizing these phenomena (the mean free path of electrons and photons, the thickness of the domain wall, critical radius of the dislocation loop, etc.). Nanostructured (nanocomposite) coatings can be divided into 3 classes according to hardness: hard nanocomposites  $H > 40$  GPa,

superhard  $40 < H > 80$  GPa, ultrahard  $H > 80-120$  GPa (the latter approach the hardness of natural diamond and BN (cubic) and higher, according to modern forecasts and calculations obtained using molecular dynamics. Therefore, an urgent task of modern materials science is the development of new multicomponent superhard coatings for multifunctional purposes, with a high level of physical and mechanical properties. These coatings, operating under load, must have high adhesion and fatigue strength, low coefficient of friction, resistance to wear and corrosion and resistance to high temperatures Promising materials as coatings operating under extreme operating conditions are micro- and nanostructured coatings based on elements such as Ti, Zr, Hf, Al, Si, N and their combinations in the form of multicomponent nitri

waters or carbonitrides, which complexly combine high physical, mechanical and tribotechnical properties and have sufficient resistance to oxidation.

### Objects And Methods of Research

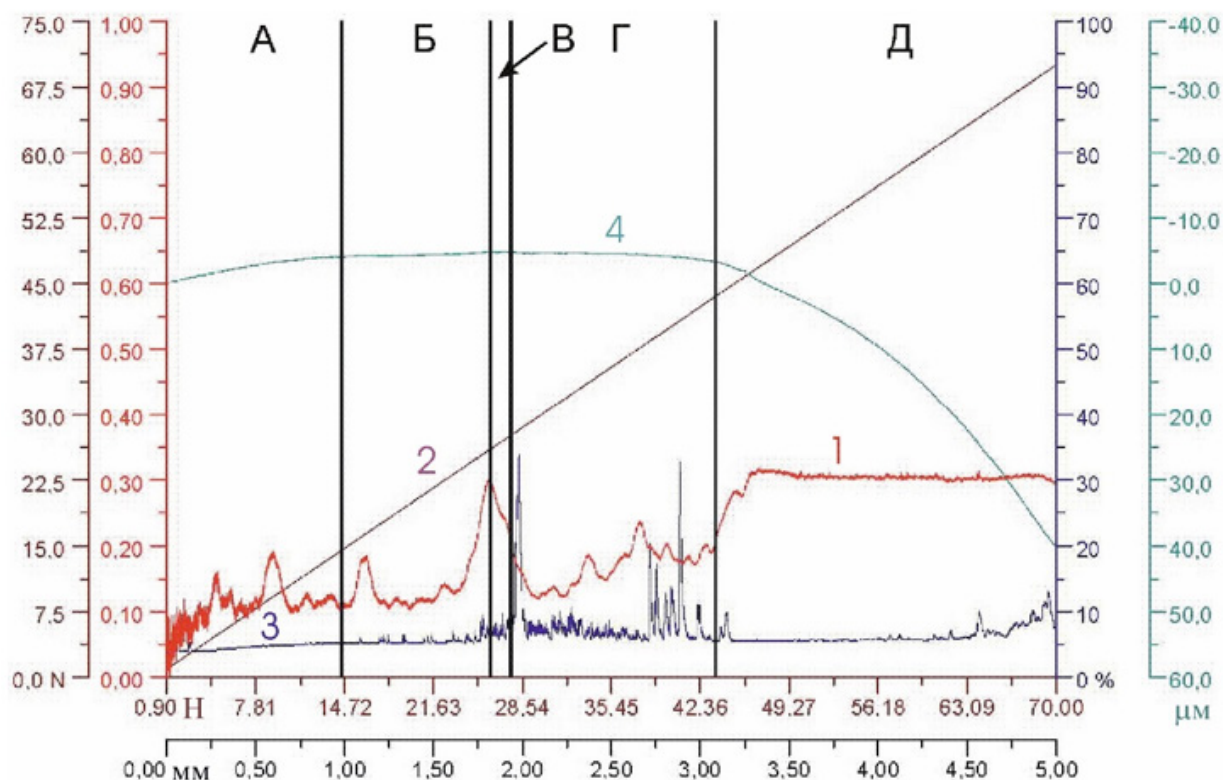
For the formation of materials used for the synthesis of coatings, all-metal cathodes based on titanium grade VT-1-00 were used; zirconium obtained by electron beam melting; silicon brand Kr00; aluminum A999; composite cathodes TiZr (75:25 at.%) and TiSi (95:5 at.%). Pure nitrogen gas ( $\leq 0.02\%$  oxygen) was used as the reaction gas. The substrates on which the coatings were applied were made in the form of steel disks (S3 steel and 12Kh18N10T steel) and plates (12Kh18N9T steel). Before coating, the substrates were polished on both sides, ultrasonically cleaned, and the surface to be coated was polished with an ion beam [3, 5].

Mechanical tests were carried out on an AFFRI DM-8 microhardness tester equipped with a Vickers indenter (four-sided diamond pyramid) and on a Nano Indenter II nanohardness tester (MTS Systems, USA) using a Berkovich indenter (trihedral diamond pyramid). These methods make it possible to study the micro- and nanomechanical behavior and structural sensitivity of the mechanical properties of near-surface layers depending on

their thickness. Tribological tests of nanocomposites were carried out according to the "ball-disk" method on a tribomachine Nano tribometer (NTR2) using a ball made of  $\text{Si}_3\text{N}_4$  as a counterbody and tribomachine CSM Instruments using ball made from  $\text{Al}_2\text{O}_3$ . The studies were carried out under dry conditions at room temperature.

### Results And Their Discussion

On Figure 1 shows the results of testing the strength of Zr-Ti-Si-N coatings of the second series before and after annealing in vacuum to a temperature of  $800^\circ\text{C}$ . For a Zr-Ti-Si-N sample in the initial state (zone A, Figure 1a), no increase in the normal load (line 2) is observed. When the normal load is increased to 25 N (zone B), the appearance of weak fluctuations of the acoustic emission signal is observed, which is not associated with the destruction of the coating, but is a consequence of the anisotropy of the coating. With a slight increase in the normal load to 27.5 N (zone B), the beginning of partial destruction of the coating is observed. Zone G is characterized by a more intense stage of crack formation, the moment of formation of which is recorded by acoustic emission peaks in the load range of 39-42 N (line 3). Zone D is associated with intense destruction of the coating and an increase in the coefficient of friction.



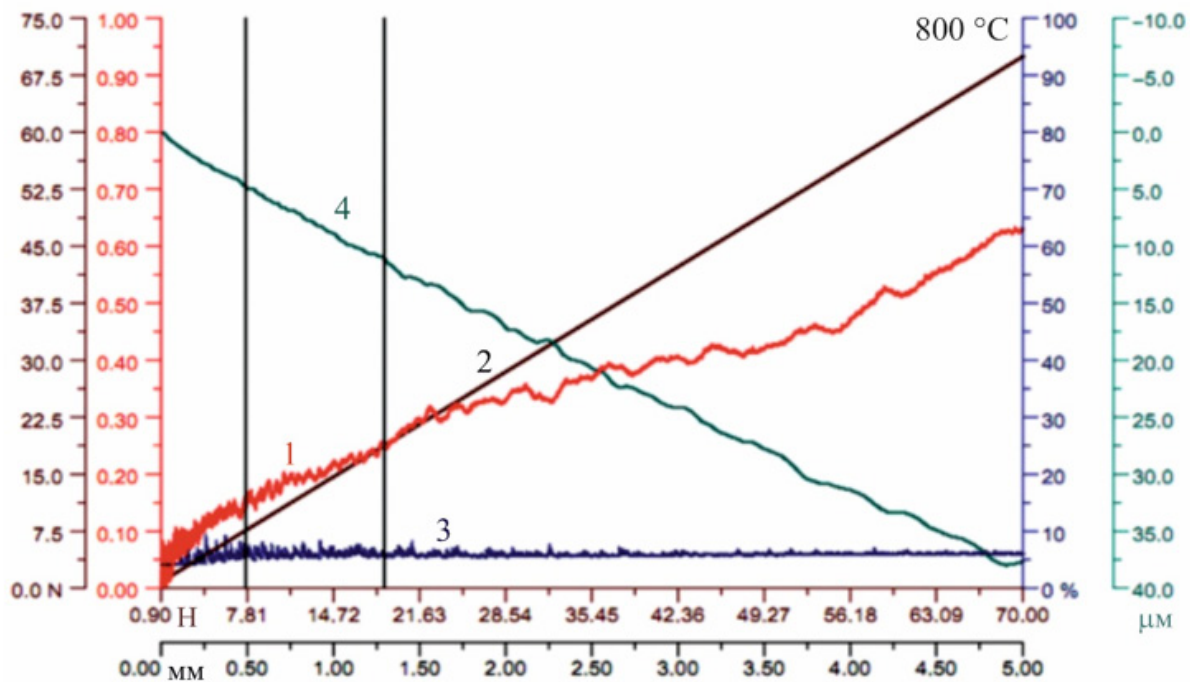


**Figure 1:** Results of measuring the adhesive strength of the Zr-Ti-Si-N coating of the second series before and after annealing in vacuum at a temperature of 800 °C. 1-friction coefficient; 2 - normal load; 3 - acoustic emission; 4 - penetration depth.

After annealing, the friction coefficient for the Zr-Ti-Si-N coating at the exit increases by about 2 times, which indicates an increase in the wear of the coating surface and leads to a deterioration in its wear resistance (Figure 1b).

The results of adhesion tests for Ti-Hf-Si-N coatings of the first series are shown in Figure 2. With an increase in the load on the indenter, the dependence of the friction coefficient on the

load acquired an oscillatory character: an increase in the friction coefficient is accompanied by a sudden flash of acoustic emission and a slowdown in the penetration of the indenter into the material. This indicates that the Ti-Hf-Si-N hard coating on the surface of the softer material (steel substrate) exhibits significant resistance to the diamond indenter until it is completely abraded under heavy loads [6, 7].

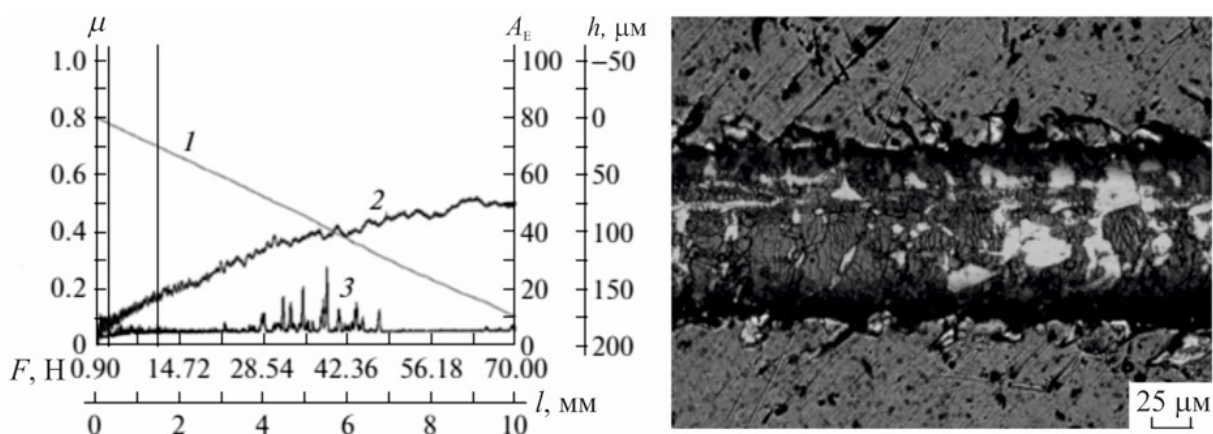


**Figure 2:** Results of measuring the adhesive strength of Ti-Hf-Si-N composite coatings of the first series (left). 1 - penetration depth ( $h$ ); 2 - coefficient of friction ( $\mu$ ); 3 - acoustic emission ( $A_e$ ) and coating structure in the destruction zone under loads in the range of 0.9-90.0 N (right).

For the Ti-Hf-Si-N sample of the third series, it was found that the friction coefficient at the initial stage is 0.12, which most likely indicates the lowest surface roughness of this coating compared to other coatings. At the next stage, after the wear of a segment 2.5 m long, the coating is destroyed (with the formation of depressions and cracks), that is, its abrasive wear occurs. As a result, the friction coefficient increases to 0.45. This value was fixed for a coating of moderate hardness ( $H = 38.3$  GPa), and, possibly, can also be associated with the presence of a quasi-amorphous  $\text{Si}_3\text{N}_4$  binder and a lower concentration of hafnium atoms in the (Ti,Hf)N solid solution.

The destruction of the Ti-Hf-Si-N coating of the first series begins with the appearance of individual chevron cracks at the bottom of the wear groove, which leads to an increase in local stresses and friction forces. This causes rapid wear of the coating (Figure 2).

Two main critical loads are determined by changing the curves of the dependences of the friction coefficient and acoustic emission on the applied load. The first corresponds to the beginning of the cohesive failure of the coating, while the second corresponds to the plastic wear of the coating (adhesive failure). Based on the results of adhesion tests, it can be argued that cohesive failure of Ti-Hf-Si-N coatings occurs at a load of 2.38 N, and adhesive failure occurs at a load of 9.81 N.

Next, we consider the results of measuring the mechanical characteristics of Zr-Ti-Si-N nanocomposite coatings obtained using a pulsed RF bias potential and comparing the obtained values with the corresponding values for ZrN, TiN, Ti-Si-N, Zr-Si-N coatings.

It is shown that silicon impurities change the hardness of Zr-Si-N and Ti-Si-N nanocomposite coatings. The hardness and modulus of elasticity of Zr-Si-N coatings and with a Si content of 8 at. % represented  $H = 43$  GPa and  $E = 474$  GPa, respectively. In comparison for ZrN coating:  $H = 32.1$  GPa,  $E = 402$  GPa; for TiN coatings:  $H = 28$  GPa and  $E = 312$  GPa; for Ti-Si-N coatings:  $H = 38-39$  GPa and  $E = 356$  GPa.

The research results indicate that the H/E ratio varies from 0.07-0.08 for ZrN and TiN, respectively, to 0.09 for nanocomposite quasi-binary Zr-Si-N coatings with Si content = 8 at. %. The values of the H/E ratio obtained as a result of research for Ti-Si-N coatings

with Si content = 8 at. % was 0.11, thus approaching the maximum possible value of 0.14 - for the amorphous state of the material. With the use of silicon as an alloying element for coatings based on ZrN and TiN, which differ in the electronic state, it seems possible to increase the hardness of the coatings.

Experimental studies have shown that the hardness of Zr-Ti-Si-N coatings before annealing, depending on the phase composition and structural state, varies from 32.4 GPa to 40.8 GPa, and the elastic modulus changes from 333 GPa to 392 GPa. After annealing of the Zr-Ti-Si-N coatings in vacuum, a partial decomposition of the solid solution occurs, the formation of an amorphous phase of silicon nitrides, which leads to the formation of a new structural-phase state, as a result of which an increase in hardness values up to 48.6 GPa (Figure 3) and an increase in the elastic modulus up to 456 GPa. The H/E ratio for Zr-Ti-Si-N nanocomposite coatings varies depending on the structural state within 0.08-0.11. This characterizes the change in the structural-phase state of coatings from finely crystalline to amorphous nanocrystalline coatings.

Further, the subsection describes the results of measuring the mechanical properties of Ti-Hf-Si-N coatings using a three-sided Berkovich diamond pyramid. It was found that the samples of the second and third series (obtained by the direct jet method) have lower hardness and elasticity modulus ( $H = 37.4-38.3$  GPa;  $E = 320-360$  GPa) compared to the corresponding values for the samples of the first and fourth series, obtained using separation of the ion-plasma flow ( $H = 42.7-48.8$  GPa;  $E = 390-520$  GPa). It is obvious that the formation of a two-phase system consisting of a substitutional solid solution (Ti,Hf)N and the  $\alpha\text{-Si}_3\text{N}_4$  phase improves the mechanical performance of Ti-Hf-Si-N coatings, making them promising for use as protective coatings.

Let us consider the results of tribological studies of Zr-Ti-Si-N nanocomposite coatings obtained using a pulsed RF bias potential, and a comparative characterization of the obtained data with the corresponding data for Ti-Si-N coatings is carried out.

Ti-Si-N nanocomposite coatings were carried out in air according to the "ball-disk" scheme at a temperature of 30°C, 300°C and 500°C. An  $\text{Al}_2\text{O}_3$  ball was used as a counterbody. The tribotechnical data obtained as a result of the tests are presented in Table 1.

**Table 1:** Results of tribological tests of nanocomposite coatings Zr-Ti-Si-N and Ti-Si-N.

Coating	Temperature	Coating wear factor, $\times 10^{-5} \text{ mm}^3 / \text{N} \cdot \text{m}$	Sample wear factor, $\times 10^{-5} \text{ mm}^3 / \text{N} \cdot \text{m}$	fmp
Zr-Ti-Si-N (1)	thirty	7.59	1.93	0.8
	300	2.22	3.14	0.71
	500	1.49	2.81	0.58
Zr-Ti-Si-N (2)	thirty	7.55	3.21	0.8
	300	1.84	4.72	0.83
	500	1.47	3.04	0.58
Zr-Ti-Si-N (3)	thirty	6.75	3.3	0.79
	300	3.62	3.83	0.81
	500	1.98	2.74	0.58
Ti-Si-N	thirty	7.69	3.28	0.88
	300	2.63	3.49	0.82
	500	1.95	2.75	0.69

It has been established that the structural-phase state of coatings plays a decisive role in wear processes. The dependence of the wear factor on temperature was also revealed. At a temperature of 30°C, as a result of tests of the adhesive interaction of the Zr - Ti - Si - N, Ti - Si - N coatings with the  $\text{Al}_2\text{O}_3$  counterbody, a rough relief of the coating surface was observed. After testing at a temperature of 300°C, the wear of the Ti-Si-N and Zr-Ti-Si-N coatings decreases, while the wear of the counterbody increases. With a further

increase in temperature to 500°C, the wear of the Ti-Si-N and Zr-Ti-Si-N coatings continues to decrease, as a result of which their durability increases. This leads to a change in the conditions of the processes occurring in the contact zone due to a change in the structure of the surface layers.

On Figure 4 shows micrographs of wear of the  $\text{Al}_2\text{O}_3$  counterbody and friction tracks on the surface of Zr-Ti-Si-N coatings.

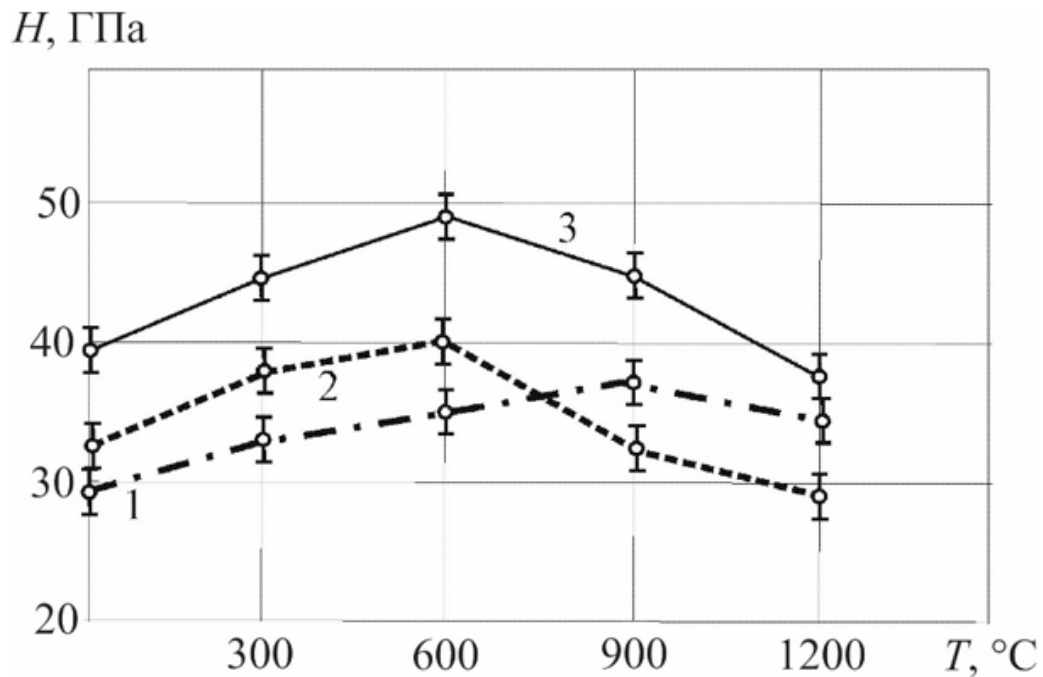


**Figure 3:** Dependence of hardness  $H$  of Zr-Si-N (1), Zr-Ti-N (2) and Zr-Ti-Si-N (3) nanocomposite coatings on annealing temperature  $T$ .

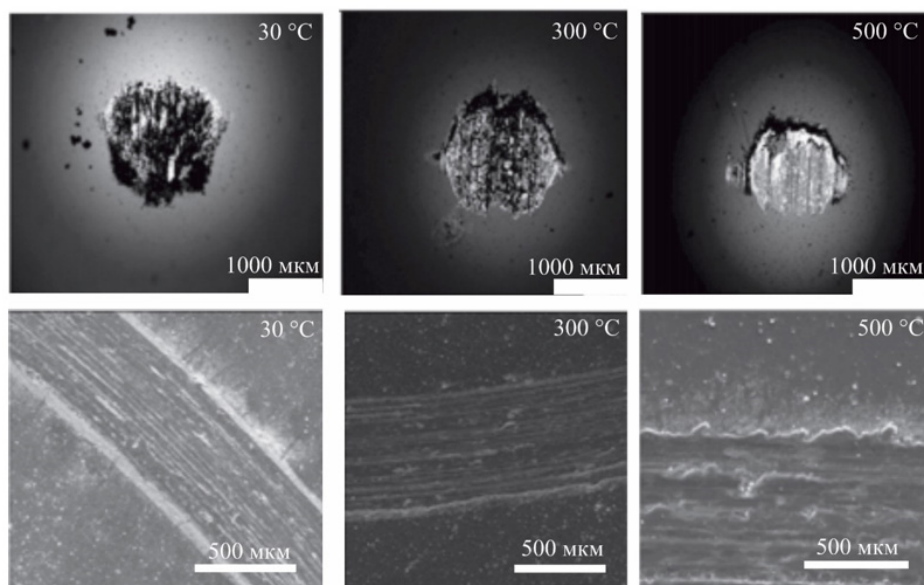


**Figure 4:** Micrographs of the surface of the counterbody after friction (top) and friction tracks (bottom) on the surface of the Zr-Ti-Si-N coating at temperatures of 30°C, 300°C, 500°C.

During friction, uniform abrasive wear of the rubbing pair was observed with the removal of wear products and their accumulation along the edges of the groove. The destruction of coatings begins with the appearance of cracks at the bottom of the wear groove, which causes an increase in local stresses and friction forces. In this case, the coating begins to wear out quickly.

### Conclusion

For the first time, a number of new micro- and nanostructured coatings based on Ti - Si - N / WC - Co - Cr were obtained by a combination of cumulative-detonation and vacuum-arc deposition methods in an RF discharge with high physical and mechanical properties, in particular, hardness  $H = 38 \div 44$  GPa and a high modulus of elasticity  $E = 420 \div 480$  GPa, as well as to achieve a reduction in coating wear by a factor of 3 compared to the original substrate. The leading role in the hardening of coatings was found - this is a decrease in the grain size from  $(25 \div 90)$  nm. up to  $(12 \div 15)$  or amorphous (quasi-amorphous) layer of  $\text{Si}_3\text{N}_4$  or the volume ratio of the second nanostructured phase.

### Acknowledgment

None.

### Conflict of Interest

None.

### References

1. Azadi M, Rouhaghdam AS, Ahangarani S, Mofidi HH, Valiei M, et al. (2013) Mechanical Behavior and Properties of TiN/TiC Coating Using PACVD. AMR.
2. N Ch Kaushik, RN Rao (2016) Effect of grit size on two body abrasive wear of Al 6082 hybrid composites produced by stir casting method, Tribology International 102: 52-60.
3. Pogdebnjak AD, Shpak AP, Beresnev VM, Kolesnikov DA, Kunitskii Yu A, et al. (2012) Effect of thermal annealing in vacuum and in air on nanograin sizes in hard and superhard coatings Zr-Ti-Si-N, Journal of nanoscience and nanotechnology 12(12): 9213-9219.
4. Umarov A V (2022) Current status and trends in the physicochemical properties of nanomaterials and nanotechnology researches, Iranian Journal of Physics Research 22(3): 67-83.
5. Pogdebnjak AD, Beresnev VM, Demyanenko AA, Bairdak VS, Komarov FF, et al. (2012) Adhesive strength, superhardness and the phase and elemental compositions of nanostructured coatings based on Ti-Hf-Si-N, Physics of the Solid State 54(9): 1882-1890.
6. Pogrebnyak AD, Bratushka SN, Il'yashenko MV, Makhmudov NA, Kolisnichenko OV, et al. (2011) Tribological and physical-mechanical properties of protective coatings from Ni- Cr-B-Si-Fe/WC-Co-Cr before and after fission with a plasma jet, Journal of Friction and Wear 32(2): 84-90.
7. Sapaev IB, Sapaev B, Umarov AV, Kamalova DI, Kasimova GA, et al. (2022) AIP Conference Proceedings 2432, 020007.